$T=0$ phase diagram and nature of domains in ultrathin ferromagnetic films with perpendicular anisotropy

Santiago A. Pighín [a], Orlando V. Billoni [a], Daniel A. Stariolo [b,1], Sergio A. Cannas [a,*]

[a] Facultad de Matemática, Astronomía y Física, Universidad Nacional de Córdoba, Instituto de Física Enrique Gaviola (IFEG-CONICET), Ciudad Universitaria, 5000 Córdoba, Argentina
[b] Departamento de Física, Universidade Federal do Rio Grande do Sul, National Institute of Science and Technology for Complex Systems, CP 15051, 91501-970 Porto Alegre, RS, Brazil

ABSTRACT

We present the complete zero temperature phase diagram of a model for ultrathin films with perpendicular anisotropy. The whole parameter space of relevant coupling constants is studied in first order anisotropy approximation. Because the ground state is known to be formed by perpendicular stripes separated by Bloch walls, a standard variational approach is used, complemented with specially designed Monte Carlo simulations. We can distinguish four regimes according to the different nature of striped domains: a high anisotropy Ising regime with sharp domain walls, a saturated stripe regime with thicker walls inside which an in-plane component of the magnetization develops, a narrow canted-like regime, characterized by a sinusoidal variation of both the in-plane and the out of plane magnetization components, which upon further decrease of the anisotropy leads to an in-plane ferromagnetic state via a spin reorientation transition (SRT). The nature of domains and walls are described in some detail together with the variation of domain width with anisotropy, for any value of exchange and dipolar interactions. Our results, although strictly valid at $T=0$, can be valuable for interpreting data on the evolution of domain width at finite temperature, a still largely open problem.

© 2010 Elsevier B.V. All rights reserved.

1. Introduction

The magnetic phases of ferromagnetic thin films with perpendicular anisotropy have been the subject of intense experimental [1–7], theoretical [8–14] and numerical [15–20] work in the last 20 years. Magnetic order in ultrathin ferromagnetic films is very complex due to the competition between several different energy contributions, the most prominent being exchange and dipolar interactions, together with a strong influence of shape and magnetocrystalline anisotropies of the sample. These in turn are very susceptible to the growth conditions of the films [21,6].

A widely used model that contains the main ingredients of ultrathin film magnetism is the 2D dimensionless Heisenberg Hamiltonian:

$$\mathcal{H} = -\delta \sum_{\langle i,j \rangle} \vec{S}_i \cdot \vec{S}_j + \sum_{(i,j)} \left[\frac{\vec{S}_i \cdot \vec{S}_j}{r_{ij}^3} - 3 \frac{(\vec{S}_i \cdot \vec{r}_{ij})(\vec{S}_j \cdot \vec{r}_{ij})}{r_{ij}^5} \right] - \eta \sum_i (S_i^z)^2 \quad (1)$$

where $\vec{S}_i$ are classical unit vectors, the exchange and anisotropy constants are normalized relative to the dipolar coupling constant ($\delta \equiv J/\Omega, \eta \equiv K/\Omega$), $\langle i,j \rangle$ stands for a sum over nearest neighbors pairs of sites in a square lattice, (i,j) stands for a sum over all distinct pairs and $r_{ij} \equiv |\vec{r}_i - \vec{r}_j|$ is the distance between spins i and j.

At low temperatures and strong enough perpendicular anisotropy, the presence of a striped phase (i.e., a modulated pattern of local perpendicular magnetization with a well defined stripe width h) is well established and is the ground state of the system [9,10,22]. In the limit of strong uniaxial anisotropy domain walls are sharp and the energy cost for deforming or moving a domain wall is large. Nevertheless, even when the mechanism by which the width of domains adjusts is not well understood, the stripe width varies with the effective anisotropy. When the thickness of the films (or the temperature) grows, the effective perpendicular anisotropy is reduced in films of a few monolayers, and magnetostatic energy becomes important, inducing the magnetization to develop an in-plane component. Domains become narrower, walls become wider and are of Bloch type at low temperatures [4,23], until the system goes through a Spin Reorientation Transition (SRT) when anisotropy and dipolar energies cancel [24–26,5]. Around the SRT line a canted state may develop, where the magnetization presents a finite in-plane component together with the perpendicular modulation. The extension of the canted state in parameter space strongly

depends on the nature of the relevant anisotropies. For some systems, like Co/Au(111), it seems necessary to go beyond the first order anisotropy approximation of the model (1). A second order anisotropy energy is responsible for a canted state in a large portion of the phase diagram [25,16,14]. For other systems, like Fe/Cu(0 0 1), the first order anisotropy seems to be enough to describe the relevant physics [27,28]. In this case, as described by the model (1), the canted state is restricted to a narrow region of parameter space around the SRT, as expected from general considerations [16], and reported in simulations at finite temperature [29]. Finally, when the dipolar anisotropy exceeds the magnetocrystalline one, the system enters an in-plane ferromagnetic state.

In this work we extend previous calculations [9,30,13] and compute the complete phase diagram in the (δ,η) space of Hamiltonian (1), at $T=0$. We also improve upon previous results by considering different kinds of domain walls (sinusoidal, hyperbolic tangent, sharp walls), as appropriate for each regime in parameter space. We consider only straight domains, (domains in which the spin orientation can be modulated along the x direction but is constant in the perpendicular direction y) separated by Bloch walls, i.e., walls in which the magnetization stays inside the yz plane. The local magnetization vector inside the domains may be tilted at an angle θ with respect to the plane normal (z-axis). Within these assumptions, we obtain the complete phase diagram, the variation of the angle θ and the behavior of the width of domains and walls in the whole parameter space (δ,η). This allows, e.g., to obtain the crossover between Heisenberg (extended walls) and Ising (sharp walls) regimes. We verify that domain width adjustment with varying anisotropy is only possible in the Heisenberg regime, domain width being fixed in the Ising regime for any value of the parameters η. Analytical calculations are complemented with Monte Carlo simulations specially designed for the present purposes, as explained in the appendix.

2. Zero temperature phase diagram

We consider a square lattice with $N=L\times L$ sites, characterized by the integer indexes (x,y), where $-L/2\leq x\leq L/2$ and $-L/2\leq y\leq L/2$, in the limit $L\to\infty$. Hence, the index i in Eq. (1) denotes a pair of coordinates (x,y). We consider only uniformly magnetized solutions along every vertical line of sites, i.e. $\vec{S}_{(x,y)}=\vec{M}(x),\forall y$ and allow only Bloch walls between domains of perpendicular magnetization, i.e. $M^x(x)=0\ \forall x$. Yafet and Gyrogy (YG) showed that for these types of spin configurations the energy per spin can be mapped onto the energy of a one dimensional XY model [9]. The energy difference between an arbitrary magnetization profile $\vec{M}(x)$ and a uniformly in-plane magnetized state is then given by

$$e[\vec{M}(x)]=(\delta-2c_2)-\frac{\delta'}{L}\sum_x\vec{M}(x)\cdot\vec{M}(x+1)+\frac{1}{L}\sum_{x,x'}\frac{M^z(x)M^z(x')}{|x-x'|^2}$$
$$-\frac{\kappa'}{L}\sum_x[M^z(x)]^2+C \tag{2}$$

where $\delta'=\delta-2c_1,\kappa'=\eta-3g,\quad c_1=0.01243\ldots,\quad c_2=0.07276\ldots,$ $g=1.202057\ldots$ and

$$C\equiv C[M^y(x)]=2(c_2-c_1)\frac{1}{L}\sum_x M^y(x)M^y(x+1) \tag{3}$$

Although small, this correction term makes a non-negligible contribution when the domain walls are of the same order of the lattice constant. This happens for small values of δ ($\delta<5$), where both stripe and wall widths are of the order of a few lattice

spacings. For larger values of δ it is reasonable to assume a smooth magnetization profile [9] $M^y(x+1)\approx M^y(x)$, so that the correction (3) can be absorbed into the anisotropy term in Eq. (2), replacing $\kappa'\to\kappa=\eta-3g+2(c_2-c_1)$.

Now consider a stripe-like periodic structure of the magnetization profile with period $2h$, $M^z(x+h)=-M^z(x)$. Using a Fourier expansion:

$$M^z(x)=M_0\sum_{m=1,3,\ldots}b_m\cos\left(\frac{m\pi x}{h}\right), \tag{4}$$

the energy (2) can be written as [9]

$$e[\vec{M};\delta,\eta]=(\delta-2c_2)-\delta'\frac{1}{L}\sum_x\cos[\phi(x)-\phi(x+1)]$$
$$+M_0^2\sum_{m=1,3,\ldots}b_m^2 D_m(h)$$
$$-\frac{\kappa'M_0^2}{2}\sum_{m=1,3,\ldots}b_m^2+C \tag{5}$$

where $\phi(x)$ is the angle between $\vec{M}(x)$ and the z-axis and

$$D_m(h)\equiv\sum_{u=1}^\infty\frac{\cos(m\pi u/h)}{u^2}=\frac{\pi^2}{6}-\frac{\pi^2 m}{2h}+\left(\frac{\pi m}{2h}\right)^2 \tag{6}$$

Now we look for the minimum of Eq. (5) for different values of δ,η. We propose different striped magnetization profiles $M^z(x)$ and compare the energies obtained by minimizing Eq. (5) for each profile with respect to variational parameters.

We first consider a profile as proposed by YG, that is constant $|M^z(x)|=M_0$ inside the stripes with a sinusoidal variation inside the walls between stripes (see Ref. [9, Fig. 1]). This will be called "sinusoidal wall profile approximation" (SWP). In order to allow for canted profiles, we take $M_0=\cos\theta$, where θ is the canting angle, i.e. we define it as the minimum angle of the local magnetization with respect to the z-axis. In Ref. [9] this variational problem was solved for $M_0=1$ in the continuum limit, i.e. when $h\gg 1$ and the wall width $w\gg 1$, so that the profile can be considered a smooth function of x. While this approximation is expected to work well for large enough values of δ, it breaks down for relatively small values of it, where the discrete character of the lattice has to be taken into account. However, the variational problem for that range of values of δ can be solved exactly (although numerically) by minimizing Eq. (5) with respect to the *integer* variational parameters h and w and continuous parameter θ. In other words, for every pair of values (δ,η) we evaluate the energy Eq. (5) for the sinusoidal profile with different combinations of $h=1,2,\ldots$ and $w=1,2,\ldots$ within a limited set. For every pair of values h,w, we look for the value of θ that minimizes the energy with a resolution $\Delta\theta=0.01$ and compare all those energies. This calculation is feasible for values up to $\delta=10$, for which the maximum value of h (bounded by the stripe width in the $\eta\to\infty$ limit) remains relatively small (smaller than $h=140$). Some results for $\delta=15$ close to the SRT were also obtained. All the results of this calculation are compared against Monte Carlo (MC) simulations. Details of the MC method used are given in Appendix A. Through these calculations we obtain a zero temperature phase diagram for low values of δ.

Before presenting the results, it is important to introduce some notations and definitions of different types of solutions. We distinguish between four types of solutions. If the minimum energy solution corresponds to $w=1$ and $\theta=0$ (within the resolution $\Delta\theta$), we call this a *Striped Ising Profile* (SIP), i.e. a square wave like profile. If $\theta=0$ but $w>1$, we call this a *Saturated State* (SS). These states only show a finite in-plane component of the magnetization inside the walls. If $0<\theta<\pi/2$ the solution is a

canted-like state. Finally, if $\theta = \pi/2$ ($M_0 = 0$) we have a *planar ferromagnet* (PF).

The zero temperature phase diagram for small values of $\delta(\delta \leq 5)$ is shown in Fig. 1. For relatively large values of η the minimum energy configuration is always the Ising one (SIP), with a stripe width independent of η. For small values of η the minimum energy configuration is the PF, with a spin reorientation transition line (SRT), either to the Ising state for $h < 3(\delta \sim 2)$ or to a canted-like one for $h \geq 3(\delta > 2)$. No Saturated State configurations are observed for $\delta < 6$.

Inside the canted region, a strong stripe width variation with the anisotropy is observed at constant δ. Note that the vertical lines that separate Ising striped states with consecutive values of h bend inside the canted region and become almost horizontal as δ increases. Hence, the exponential increase of h with δ in the Ising region (vertical lines) changes to an exponential increase with η inside the canted region (curved lines on the right of Fig. 1). It is important to note here that the canted region in this system corresponds almost everywhere (except close to the crossover to an Ising striped state) to a regime in which the stripe width and walls are almost equal, which means a pure sinusoidal magnetization profile. In this sense it has a different character than the "true" canted phases obtained in systems with non-zero higher order anisotropies [16,14], where well defined domains show a finite in-plane magnetization component. In the present case the canted like states are characterized by a sinusoidal variation (with wave length $2h$) in both the in-plane and the out of plane magnetization components, without well defined domains (see an example in Fig. 3). Hence, there are not truly "stripes", but a sinusoidal modulated state or Single Mode Canted Profile (SMCP).

We also find an excellent agreement between the sinusoidal wall approximation (or SMCP) and the MC results, except close to the transition between the Ising and the canted-like states. Such disagreement is due to the fact that the actual wall is not well described by a sinusoidal profile far away of the SRT line, as will be shown later.

For large enough values of δ the variational problem for the SWP can be solved in a continuum approximation introduced by YG [9], giving a set of coupled non-linear equations for the stripe width h, the ratio between the stripe and the wall widths $\Delta = w/h$ and the canted angle θ. In the limit $\Delta \to 1$ those equations can be solved analytically predicting a SRT at the line [9]

$$\eta_{SRT}(\delta) = a - \frac{\pi^2}{2\delta} \qquad (7)$$

with $a = \pi^2/3 + 3g - 2(c_2 - c_1)$. The line Eq. (7) is also depicted in Fig. 1. Notice the disagreement between the continuum approximation and the exact one for $\delta \leq 5$. This discrepancy becomes smaller than 1% only for $\delta > 7$.

For arbitrary values of η and δ the equations for h, Δ and θ can be solved numerically. From the numerical solutions we found that the range of values of the anisotropy η for which the canted angle is appreciable different from zero within this approximation is strongly depressed as δ increases. For values $\delta \sim 100$ the canted-like configurations almost disappear, except very close to the reorientation line, as already reported by Politi [13].

Indeed, from our MC simulations, we observe that the range of values for which canted-like states have the minimum energy gradually shrinks as δ increases, being replaced by a saturated state for values of η above certain threshold. This can be observed in Fig. 2, where we show the behavior of the canted angle and the in-plane magnetization component $M_{\parallel} = (1/L)\sum_x M^y(x)$ as a function of η for $\delta = 7.5$. The Monte Carlo data show the existence of a wide range of values of η for which the canted angle is zero while $M_{\parallel} \neq 0$, meaning that the non-null in-plane components are concentrated inside the walls. In other words, in that region we have a saturated state with thick walls $w > 1$. Notice also that the SWP approach completely fails to describe those states. Moreover, we observe from our MC simulations that the SWP cease to be the minimum energy solution for values of η relatively close to the SRT, before the saturated state sets up (see Fig. 2). This effect becomes more marked as δ increases.

The departure of the magnetization profile from the SWP for large values of η and δ is expected from micromagnetic theory, which in that limit predicts that the wall structure will be dominated by the interplay between anisotropy and exchange, leading to an hyperbolic tangent shape of the wall [23]. Hence we considered a periodic magnetization profile with hyperbolic tangent walls (HWP) defined, for a wall centered at $x = 0$, by

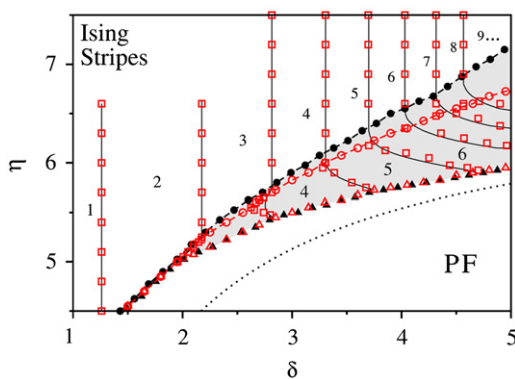$$M^z(x) = M_0 \tanh\left(\frac{x}{l_w}\right) \quad \text{for } -h/2 \leq x \leq h/2 \qquad (8)$$

Fig. 1. Zero temperature phase diagram for small values of δ. Black filled symbols and black solid lines: MC simulations. Open red symbols: SWP approximation. Squares and continuous black lines correspond to transition lines between striped states of different width. The shaded region corresponds to a canted-like state ($0 < \theta < \pi/2$). Triangles are transition lines between planar ferromagnet ($\theta = \pi/2$) and SMCP states (spin reorientation transition line). Circles mark transitions between the canted-like and the striped Ising state ($\theta = 0$ and $w = 1$). Notice the excellent agreement between the MC and SWP calculations close to the SRT, while the SWP approach underestimates the transition line between the canted-like and Ising stripes states. The dotted line corresponds to the continuum approximation of YG for the SRT (Eq. (7)). (For interpretation of the references to color in this figure legend, the reader is referred to the web version of this article.)
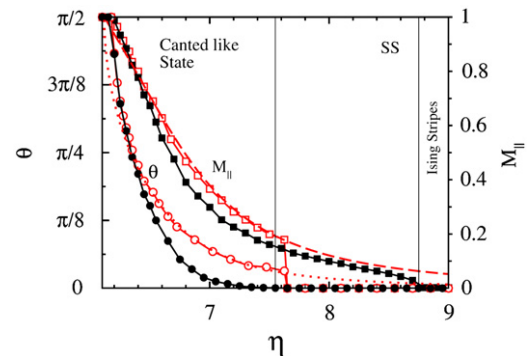

Fig. 2. Canted angle (circles) and in-plane magnetization (squares) as a function of η for $\delta = 7.5$. Filled black symbols correspond to MC calculation. Open red symbols corresponds to the discrete SWP approximation, while the red doted and dashed lines correspond to the continuum (YG) approximation of the SWP. Continuous black and red lines are only a guide to the eye. (For interpretation of the references to color in this figure legend, the reader is referred to the web version of this article.)

where $M_0 = \cos\theta$ as before. In the large δ limit, assuming a smooth profile $h \gg 1$ and $l_w \gg 1$, the anisotropy energy can be expressed as

$$e_{an} \approx -\kappa M_0^2\left[1 - \frac{2l_w}{h}\tanh\left(\frac{h}{2l_w}\right)\right] \tag{9}$$

The exchange energy can be obtained in a similar way:

$$e_{exc} = -\delta\left[1 - \frac{l_w}{h}\left(\frac{M_0^2-1}{M_0}\tanh^{-1}\left(M_0\tanh\left(\frac{h}{2l_w}\right)\right) + \tanh\left(\frac{h}{2l_w}\right)\right)\right] \tag{10}$$

The dipolar energy can be calculated using Eq. (6). The Fourier coefficients for the profile (8) can be computed using the approximation

$$\tanh(x) \approx \begin{cases} x\left(1 - \dfrac{x^2}{3}\right) & \text{if } 0 \le x \le \dfrac{1}{2} \\ (1-e^{-2x})^2(1+e^{-4x}) & \text{if } \dfrac{1}{2} \le x \end{cases} \tag{11}$$

This leads to an expression for the total energy as a function of the variational parameters h, θ and l_w that can be minimized numerically. Comparing the minimum energy solution for the SWP and the HWP we obtain the crossover line between sinusoidal and hyperbolic wall structure shown in Fig. 3 (dashed line). Above that line the HWP has always less energy than the SWP. We also calculated the transition line between the canted-like and the saturated states by setting the condition $\theta = 0.01$, to be consistent with the criterium used in the MC calculations. The results are shown in Fig. 3 together with the SRT line Eq. (7), and compared with MC calculations up to $\delta = 15$. The excellent agreement with the MC results gives support to the analytic approximations. Only between the dashed and the continuous lines we found truly canted states (i.e., states with $h \ll w$), although they parallel component is rather small ($\theta < 0.1$). In this sense, the region enclosed by both lines marks a crossover between the SMCP and the Saturated states: as η increases domains emerge gradually, the walls change from sinusoidal to hyperbolic shape and the canted angle goes to zero.

For large values of η the exponential increase of h makes it cumbersome to apply the previous approximation for the calculation of the dipolar energy. Instead of that, we can use the following heuristic argument to obtain a reasonable approximation. The main error introduced by the SWP approach is in the

Fig. 3. Zero temperature phase diagram for large values of δ. The shaded region corresponds to the canted-like states. Symbols correspond to MC simulations and lines to theoretical results. The dashed line correspond to the crossover between sinusoidal and hyperbolic wall structure. The lower line (blue) corresponds to Eq. (7). The middle line (red) is obtained from the HWP minimum energy solution with $\theta = 0.01$. The upper line (black) corresponds to Eq. (19). Typical magnetization profiles obtained by MC are shown for every region of the phase diagram. (For interpretation of the references to color in this figure legend, the reader is referred to the web version of this article.)

exchange and anisotropy contributions to the energy. Since the main contribution to the dipolar energy is given by the interaction between domains, we can assume that the dipolar contribution of the wall is relatively independent of its shape. Hence, we approximate the dipolar contribution by the SWP expression obtained by YG [9] taking $w = fl_w$ (f is a fitting parameter of order one to be fixed later) in the limit $\Delta \ll 1$ ($l_w/h \ll 1$). We compare the energy obtained within this approximation with that obtained using the Eq. (11) for different values of the system parameters. We verified that the error made by taking $f = 4$ is always smaller than 1% for $h/l_w \ge 20$. We also observe that the best agreement with the MC results is obtained for $f = 4$. Assuming then $M_0 = 1$, the total energy per spin (relative to the parallel magnetized state) for the HWP can then be approached by

$$e_{HWP} = \gamma + \frac{\delta/l_w - 2l_w\gamma}{h} - \frac{4}{h}\ln\left(\frac{3\pi h}{10 l_w}\right) \tag{12}$$

with $\gamma = \pi^2/3 - \kappa$. Minimizing Eq. (12) with respect to the variational parameters h and l_w leads to:

$$h = \frac{10}{3\pi}l_w\exp\left[\frac{\delta}{2l_w}\right] \tag{13}$$

with

$$l_w = \frac{\delta}{2 + \sqrt{4 + 2(\kappa - \pi^2/3)\delta}} \tag{14}$$

in agreement with a derivation made by Politi [13].

With the previous calculation we can also estimate the transition line between the saturated and the Ising striped state. In the large h limit the energy for a SIP, i.e. for

$$\phi(x) = \begin{cases} 0 & \text{if } 0 \le x \le h/2 \\ \pi & \text{if } h/2 < x \le h \end{cases} \tag{15}$$

the energy can be easily calculated from Eq. (5). The Fourier coefficients are

$$b_m = (-1)^{(m-1)/2}\frac{4}{\pi m} \tag{16}$$

Using Eq. (6) the dipolar energy is then given by

$$e_{dip} \sim \frac{\pi^2}{3} - \frac{8}{h}\sum_{m=1,3,\ldots}^{2h-1}\frac{1}{m} + \frac{4}{h} \sim \frac{\pi^2}{3} + 4\frac{\psi(h) - \beta}{h} \tag{17}$$

where $\beta \equiv \gamma_e + \ln 4 - 1, \gamma_e \approx 0.577216$ is the Euler gamma constant and $\psi(x)$ is the digamma function [31]. The energy per spin respect to the in-plane magnetized state is then given by

$$e_I = -\kappa' + \frac{\pi^2}{3} + \frac{2\delta' - \beta}{h} - \frac{4\psi(h)}{h} \tag{18}$$

Minimizing Eq. (18) with respect to h leads to the equation $\delta'/2 - \beta = F(h)$, where $F(h) = \psi(h) - h\psi'(h) \sim \ln h - 1$, thus recovering the known result $h \sim e^{\delta/2}$. Comparing the energies, we find that the HWP has less energy than the Ising state for any value of η. Eq. (13) shows that the stripe width variation in the Saturated state is determined by the change in the wall width as the anisotropy increases. Hence, h will change until the wall width reaches the atomic limit, i.e. for $l_w = 1$, where Eq. (13) recovers the Ising behavior $h \sim e^{\delta/2}$. Imposing the condition $l_w = 1$ to Eq. (14) we obtain the transition line between the Saturated and the Ising Stripes states:

$$\eta = \frac{1}{2}\delta - 2 + \frac{\pi^2}{3} + 3g - 2(c_2 - c_1) \tag{19}$$

which is also shown in Fig. 3, in complete agreement with the MC results.

In Fig. 4 we compare the equilibrium stripe width h as a function of η obtained within the different approximations used
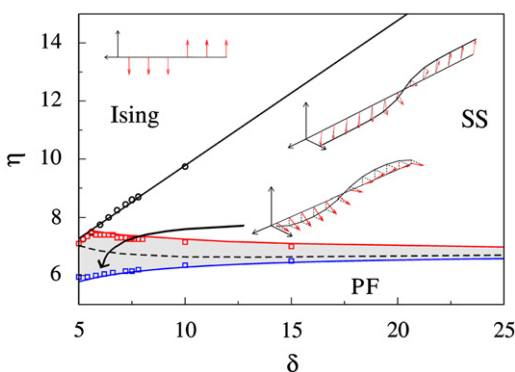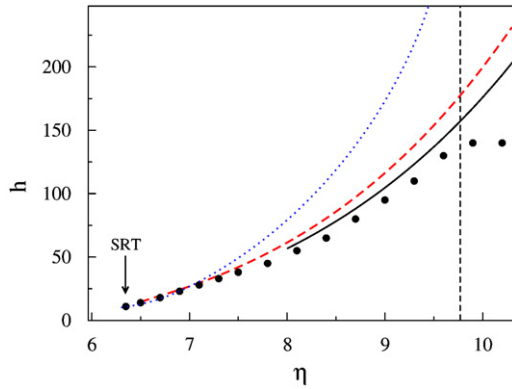
Fig. 4. Comparison of the $T=0$ stripe width h vs. η obtained within the different methods for $\delta=10$. Symbols correspond to MC simulations. Full black line corresponds to the asymptotic approximation for the HWP given by Eqs. (13) and (14). The red dashed line corresponds to the variational solution of Eqs. (9) and (10) using the approximation (11) for the Fourier coefficients in the dipolar energy. The blue dotted line corresponds to the continuous SWP. The vertical dashed line corresponds to the transition between Saturated and Ising Stripes states given by Eq. (19). (For interpretation of the references to color in this figure legend, the reader is referred to the web version of this article.)

in this work for $\delta=10$ and with the MC simulations. Notice that the asymptotic approximation for the HWP given by Eqs. (13) and (14) shows a better agreement with the MC results than the approximation (11) for the Fourier coefficients in the dipolar energy. This is because we adjusted the fitting parameter f to optimize the agreement with the MC results at low values of δ. The discrepancy between both (hyperbolic) approximations becomes negligible in the large δ limit.

3. Discussion and conclusions

The main results of this work are summarized in Figs. 1 and 3, which display the complete zero temperature phase diagram of the model defined by the Hamiltonian (1). Working upon reasonable assumptions for the ground states, like perfectly straight modulations in one dimension and Bloch domain walls, we analyzed minimum energy configurations combining a variational analysis with Monte Carlo results. We found four qualitatively different kinds of solutions: a planar ferromagnet for small anisotropies, a Single Mode Canted Profile (characterized by a sinusoidal variation of both components of the magnetization and varying wave length) close to the SRT and two types of perpendicular striped states for large values of the anisotropy: a saturated state in which the in-plane component is restricted to the domain walls, and an Ising stripe state with sharp walls for very large anisotropies.

The SMCP and saturated states give valuable information on the behavior of the stripe width (or the wave length in the SMCP case) as the anisotropy and exchange parameters change. We find that stripe width variation is directly associated to the presence of finite width domain walls. For large enough values of the anisotropy η the ground state of the system is always an Ising striped state, no matter the value of the exchange coupling δ. In those states domain walls are sharp, the stripe width is completely independent of η and grows exponentially with the exchange coupling.

At the SRT the system passes through canted-like states (mostly SMCP) as the anisotropy increases, although the range of values of η where the canted angle is different from zero narrows as δ increases. For instance, the exchange to dipolar coupling ratio in fcc Fe based ultrathin films can be roughly

estimated to be $\delta\sim100$ (considering a cubic bilayer of Fe/Cu(1 0 0), where [4] the exchange coupling $J_{Fe}\sim30$ meV, the lattice constant $d_{Fe}\sim2$ ML and [32] $\mu_{Fe}\sim3\mu_{B}$). For $\delta\sim100$ the anisotropy interval for the canted-like states is approximately $\Delta\eta=\eta-\eta_{SRT}\approx0.2$.

For $\delta<6$ the SMCP has the minimum energy in a rather extended region of the phase parameters space, close to the SRT. The wave length (or "stripe width") of those states presents a strong variation with the anisotropy, directly correlated with an increasing canted angle. According to YG approximation, SMCP solutions are expected only close to the SRT. We found that the magnetization profile maintains the sinusoidal shape as the anisotropy increases. Above certain value of η the wall profile changes to a hyperbolic tangent shape, while the magnetization inside the domains becomes fully saturated.

For $\delta>6$ the ground state is given by the Saturated State, except very close to the SRT. A similar effect (i.e. a crossover between a sinusoidal and a saturated magnetization profile) has been observed in room temperature grown fcc Fe/Cu(1 0 0) ultrathin films, as the temperature decreases from T_c, even though those systems do not present SRT [33].

In the Saturated state, the stripe width increase with η is directly related to the wall width decrease through the relation $h\sim e^{\delta/2l_w}$. The wall width in turn is determined by the competition between exchange and anisotropy. Once the anisotropy is large enough that the wall width reaches the atomic limit, h growth stops. One may wonder whether a similar mechanism could be behind the stripe width variation with temperature, where a saturation is observed at low temperatures. Nevertheless, in this case other effects, like extremely slow relaxation can be responsible for the observed saturation.

Besides its direct application to real systems, knowing the ground state of this system for arbitrary values of the exchange coupling is of fundamental importance to have a correct interpretation of Monte Carlo simulation results. Being one of the most powerful tools to analyze these kind of systems at the present (specially at finite temperatures), it is basically limited by finite size restrictions, which implies relatively small values of δ (the characteristic length h of the problem grows exponentially with δ at low temperatures).

Appendix A. Zero temperature Monte Carlo technique for striped domain patterns

In order to have an independent computation of the striped profiles which minimize the energy, we implemented Monte Carlo simulation with a simulated annealing protocol and Metropolis algorithm. To compare against the analytical solutions we looked for minimum energy magnetization profiles among those characterized by periodic straight domains with Bloch walls. Hence, the problem is basically one dimensional and we could restrict the search to one dimensional patterns over the x direction fixing $S_i^x=0$ $\forall i$ and imposing periodic boundary conditions (PBC) in both the x and y directions. In other words, we simulated a lattice with $L_x\times L_y$ with $L_y=1$ and PBC, which are implemented by means of the Ewald sums technique.

The temperature was then decreased down to very low temperatures at a constant rate $T(t) = T_0 - rt$, where time is measured in Monte Carlo Steps, T_0 is the initial temperature and r is the cooling rate. For all the range of parameters of this work, we chose $T_0 = 1$ and $r = 10^{-4}$ and the simulation protocol was repeated 100 times using different sequences of random numbers in order to minimize the possibility of trapping in local minima. The results were independent of the initial spin configuration we choose at T_0. For every set of values of (δ, η) we checked the results for different values of L_x in order to avoid artificial frustration. We also performed some comparisons with MC results in a square $L_x = L_y$ lattice with PBC using the same annealing protocol and the results were indistinguishable. This ansatz allowed us to obtain MC results for values of δ up to $\delta = 10$ (for which the maximum equilibrium value is $h = 140$).

References

[1] R. Allenspach, M. Stampanoni, A. Bischof, Phys. Rev. Lett. 65 (1990) 3344.
[2] A. Vaterlaus, C. Stamm, U. Maier, M.G. Pini, P. Politi, D. Pescia, Phys. Rev. Lett. 84 (2000) 2247.
[3] O. Portmann, A. Vaterlaus, D. Pescia, Nature 422 (2003) 701.
[4] Y.Z. Wu, C. Won, A. Scholl, A. Doran, H.W. Zhao, X.F. Jin, Z.Q. Qiu, Phys. Rev. Lett. 93 (2004) 117205.
[5] C. Won, Y.Z. Wu, J. Choi, W. Kim, A. Scholl, A. Doran, T. Owens, J. Wu, X.F. Jin, H.W. Zhao, et al., Phys. Rev. B 71 (2005) 224429.
[6] C.A.F. Vaz, J.A.C. Bland, G. Lauhoff, Rep. Prog. Phys. 71 (2008) 056501.
[7] R. Frömter, H. Stillrich, C. Menk, H.P. Oepen, Phys. Rev. Lett. 100 (2008) 207202 (p. 4).
[8] J.A. Cape, G.W. Lehman, J. Appl. Phys. 42 (1971) 5732.
[9] Y. Yafet, E.M. Gyorgy, Phys. Rev. B 38 (1988) 9145.
[10] R. Czech, J. Villain, J. Phys.: Condens. Matter 1 (1989) 619.
[11] D. Pescia, V.L. Pokrovsky, Phys. Rev. Lett. 65 (1990) 2599.
[12] A. Abanov, V. Kalatsky, V.L. Pokrovsky, W.M. Saslow, Phys. Rev. B 51 (1995) 1023.
[13] P. Politi, Cond. Matter Phys. 18 (1998) 191 (Comments).
[14] V. Zablotskii, W. Stefanowicz, A. Maziewski, J. Appl. Phys. 101 (2007) 113904.
[15] K. De'Bell, A.B. MacIsaac, J.P. Whitehead, Rev. Mod. Phys. 72 (2000) 225.
[16] E.Y. Vedmedenko, H.P. Oepen, J. Kirschner, Phys. Rev. B 66 (2002) 214401.
[17] S.A. Cannas, D.A. Stariolo, F.A. Tamarit, Phys. Rev. B 69 (2004) 092409.
[18] S.A. Pighín, S.A. Cannas, Phys. Rev. B 75 (2007) 224433.
[19] L. Nicolao, D.A. Stariolo, Phys. Rev. B 76 (2007) 054453.
[20] M. Carubelli, O.V. Billoni, S.A. Pighín, S.A. Cannas, D.A. Stariolo, F.A. Tamarit, Phys. Rev. B 77 (2008) 134417.
[21] O. Portmann, Micromagnetism in the Ultrathin Limit, Logos Verlag, 2006.
[22] B. Kaplan, G.A. Gehring, J. Magn. Magn. Mater. 128 (1993) 111.
[23] G. Bertotti, Hysteresis in Magnetism, Academic Press, 1998.
[24] A. Moschel, K.D. Usadel, Phys. Rev. B 51 (1995) 16111.
[25] Y. Millev, J. Kirschner, Phys. Rev. B 54 (1996) 4137.
[26] R. Zdyb, E. Bauer, Phys. Rev. B 67 (2003) 134420.
[27] J.G. Gay, R. Richter, Phys. Rev. Lett. 56 (1986) 2728.
[28] W. Platow, A.N. Anisimov, M. Farle, K. Baberschke, Phys. Stat. Sol. (a) 173 (1999) 145.
[29] J.P. Whitehead, A.B. MacIsaac, K. De'Bell, Phys. Rev. B 77 (2008) 174415.
[30] A.B. MacIsaac, K. De'Bell, J.P. Whitehead, Phys. Rev. Lett. 80 (1998) 616.
[31] I.S. Gradshteyn, I.M. Ryzhik, Table of Integrals, Series and Products, fifth ed., Academic Press, 1994.
[32] J.H. Dunn, D. Arvanitis, N. Mårtensson, Phys. Rev. B 54 (1996) R11157.
[33] A. Vindigni, N. Saratz, O. Portmann, D. Pescia, P. Politi, Phys. Rev. B 77 (2008) 092414.